

MIT Open Access Articles

Toward a Germanium Laser for Integrated Silicon Photonics

The MIT Faculty has made this article openly available. **Please share** how this access benefits you. Your story matters.

Citation: Kimerling, L.C., and J. Michel, with Xiaochen Sun and Jifeng Liu. "Toward a Germanium Laser for Integrated Silicon Photonics." Selected Topics in Quantum Electronics, IEEE Journal Of 16.1 (2010) : 124-131. © 2010 IEEE.

As Published: <http://dx.doi.org/10.1109/jstqe.2009.2027445>

Publisher: Institute of Electrical and Electronics Engineers

Persistent URL: <http://hdl.handle.net/1721.1/62164>

Version: Final published version: final published article, as it appeared in a journal, conference proceedings, or other formally published context

Terms of Use: Article is made available in accordance with the publisher's policy and may be subject to US copyright law. Please refer to the publisher's site for terms of use.



Toward a Germanium Laser for Integrated Silicon Photonics

Xiaochen Sun, *Member, IEEE*, Jifeng Liu, *Member, IEEE*, Lionel C. Kimerling, *Member, IEEE*, and Jurgen Michel

(Invited Paper)

Abstract—It has been demonstrated theoretically and experimentally that germanium, with proper strain engineering and n-type doping, can be an efficient light emitter and a gain medium at its direct bandgap within the third optical communication window (~ 1520 – 1620 nm). In this paper, we systematically discuss the effect of strain, doping, and temperature on the direct-gap optical gain in germanium. For electrically pumped devices, properties and design guidelines of Ge/Si heterojunction are also analyzed and compared with the results from fabricated Ge/Si heterojunction LEDs.

Index Terms—Integrated optoelectronics, light emitters, silicon photonics.

I. INTRODUCTION

SILICON-BASED optical communication and integrated optoelectronics calls for high-volume integration of laser sources at a low cost. So far, lasers on Si still rely on III–V materials either grown on or bonded to Si [1], [2]. However, considering a high-volume application, neither of these approaches will be able to supply the necessary technology for on-chip single-wavelength or wavelength-division multiplexing (WDM) laser sources. The issues are reliability, throughput, and yield. Epitaxial III–V lasers on Si still suffer limited lifetime and they involve elaborate growths of thick buffer layers, while III–V wafer bonding on Si cannot be achieved at a wafer level for industrial applications due to the size mismatch between Si and III–V substrates. As more and more wavelengths are required on-chip for WDM applications, bonding of laser chiplets becomes unfeasible. Furthermore, III–V lasers show yields that are significantly lower than required for Si CMOS processes. Therefore, a materials system that allows large-scale processing on a CMOS platform with the required emission bandwidth for WDM is crucial for the success of electronic–photonics integration on Si.

In 2007, Liu *et al.* theoretically demonstrated that, with proper band structure engineering using in-plane tensile stress and n-type doping, germanium can be used for efficient light emission and optical gain can be achieved at its direct bandgap energy

near 0.8 eV (1550 nm) [3]. Since then, there has been an increasing interest in germanium light emission research. The n-type doping-induced enhancement in room-temperature direct-gap photoluminescence from germanium has been observed and studied [4]–[6]. Onset of net gain from germanium at its direct-gap energy has also been demonstrated using pump-probe measurements [7]. A Ge/Si heterojunction LED has been fabricated and room-temperature direct-gap electroluminescence (EL) has been observed [8]. Enhanced photoluminescence has also been observed from germanium ring resonators [9]. All these results indicate that it is possible to achieve monolithically integrated Ge lasers on Si using CMOS processes for high-volume applications. In this paper, we systematically discuss the effects of strain, doping, and temperature on the direct-gap optical gain in germanium and present design rules for Ge light emitters based on the direct bandgap transition.

Germanium is normally recognized as a poor light-emitting material due to its indirect band structure. The radiative recombination through the indirect band-to-band optical transition is slow as a result of a phonon-assisted process. The indirect radiative recombination is generally inefficient since most of the injected carriers recombine nonradiatively unless the nonradiative recombination is suppressed at cryogenic temperature. The direct band-to-band optical transition in germanium, on the other hand, is a very fast process with a radiative recombination rate five orders of magnitude higher than that of the indirect transition [10]; thus, the direct-gap light emission of germanium is, in principle, as efficient as that of direct-gap III–V materials. The challenge is that the number of the injected electrons for the direct optical transition is deficient because most of the injected electrons occupy the low-energy indirect L valleys. Fortunately, germanium is a pseudodirect bandgap material because of the small energy difference (0.136 eV) between its direct bandgap and indirect bandgap. As mentioned before, it has been shown theoretically and experimentally that strained n^+ Ge can be an efficient light emitter and a gain medium at its direct-gap wavelength near 1600 nm. In the next two sections, we follow the work in [3] and discuss in more detail the characteristics of the direct-gap optical gain in germanium. In Section IV, some properties and design guidelines of Ge/Si heterojunction light emitters are discussed.

II. DIRECT BANDGAP GERMANIUM

Band structure is correlated with the crystal lattice that can be altered by strain. Tensile strain makes germanium more direct

Manuscript received May 28, 2009; revised June 24, 2009. First published October 13, 2009; current version published February 5, 2010. This work was supported by the Silicon-Based Laser Initiative of the Multidisciplinary University Research Initiative (MURI) sponsored by the Air Force Office of Scientific Research (AFOSR).

The authors are with the Microphotonics Center, Massachusetts Institute of Technology, Cambridge, MA 02139 USA (e-mail: sunxc@mit.edu; jmichel@mit.edu).

Color versions of one or more of the figures in this paper are available online at <http://ieeexplore.ieee.org>.

Digital Object Identifier 10.1109/JSTQE.2009.2027445

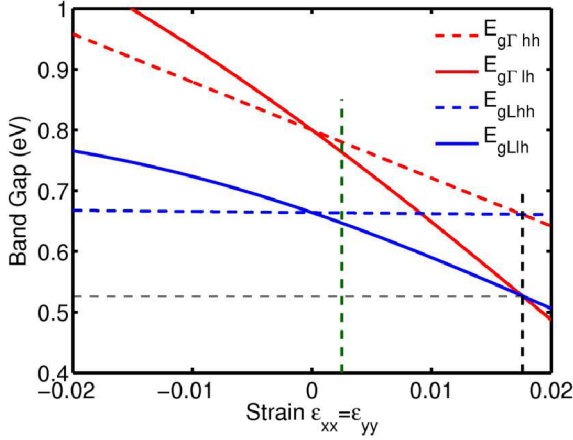


Fig. 1. Energy gaps of germanium under in-plane strain. $E_{g\Gamma hh}$ and $E_{g\Gamma lh}$ are energy gaps between the direct Γ valley and the heavy-hole band and the light-hole band, respectively. E_{gLhh} and E_{gLlh} are energy gaps between the indirect L valley and the heavy-hole band and the light-hole band, respectively.

bandgap like because it shrinks the direct bandgap more than the indirect bandgap of germanium as a result of the difference in deformation potentials of the direct Γ valley and the indirect L valleys. The direct and indirect energy gaps of germanium as a function of in-plane strain is plotted in Fig. 1. Four energy gaps are shown in the figure because tensile strain separates the degenerate light-hole band and heavy-hole band in germanium. $E_{g\Gamma hh}$ and $E_{g\Gamma lh}$ are energy gaps between the direct Γ valley and the heavy-hole band and the light-hole band, respectively. E_{gLhh} and E_{gLlh} are energy gaps between the indirect L valley and the heavy-hole band and the light-hole band, respectively. The deformation potential data used in this calculation are adopted from [11] and [12].

Fig. 1 shows that germanium becomes a complete direct bandgap material at a tensile strain of 1.8% (marked by a vertical dashed black line) and above. The large lattice mismatch between germanium and some III–V materials such as $\text{In}_x\text{Ga}_{1-x}\text{As}$ has been used to achieve high tensile strain in germanium [13], though further improvement of the optical properties is needed to achieve efficient light emission. In addition, the thickness of a pseudomorphic epitaxial film is limited by the critical thickness, which is too thin for useful devices in many applications. Instead, thermal expansion mismatch between germanium and silicon substrate has been successfully used to introduce tensile strain in germanium due to the large difference in the thermal expansion coefficient between germanium and silicon [14]–[17]. Thermally accumulated tensile strain is not limited by critical thickness, and more than 2- μm -thick tensile-strained epitaxial germanium films have been grown as an active medium in photodetectors with improved performance in the telecommunication wavelength bands [18], [19]. By using this approach, 0.25% tensile strain (marked with vertical dashed green line) has been achieved in epitaxial germanium films with a low threading dislocation density of $2 \times 10^7 \text{ cm}^{-2}$ [20]. The strain is taken into consideration in the modeling work in the next section.

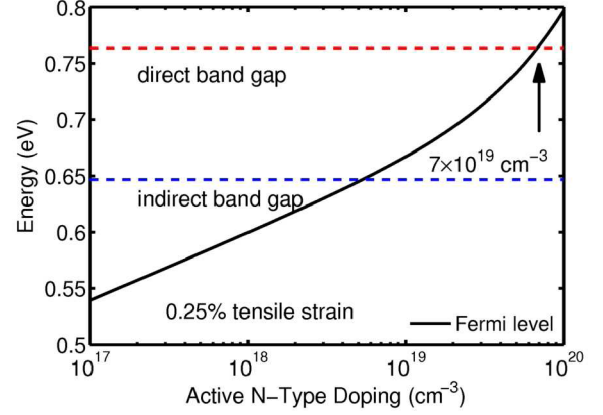


Fig. 2. Equilibrium Fermi level at room temperature as a function of active n-type doping concentration in 0.25% tensile-strained germanium. The maximum of the valence band (light-hole band) is chosen as the zero energy reference.

Too much strain-induced bandgap shrinkage can lead to a practical disadvantage in terms of emission wavelength. Tensile strain of 1.8% shrinks the bandgap (both the direct bandgap and the indirect bandgap) of germanium to 0.53 eV, thus shifting the light emission wavelength to beyond 2300 nm, far away from the telecommunication standard wavelength bands near 1550 nm at which many existing discrete or integrated photonic devices are designed to work. On the other hand, a moderate tensile strain of 0.25% only shrinks the direct bandgap from 0.8 eV (1550 nm) to 0.76 eV (1630 nm), which can cover both C and L bands (1528–1620 nm) in terms of light emission depending on the injection level, as will be explained later.

With less tensile strain, germanium does not completely become a direct bandgap material. Therefore, additional effects are needed for efficient direct-gap light emission. Doping germanium with n-type impurities is a way to solve this problem. At equilibrium, extrinsic electrons thermally activated from donor levels occupy the lowest energy states in the indirect L valleys. The calculated equilibrium Fermi level as a function of active n-type doping concentration in 0.25% tensile-strained germanium is shown in Fig. 2. Fermi statistics is used in the calculation to accurately describe the heavily doped, degenerate material. It can be seen that the Fermi level raises to the minimum of the direct Γ valley at a doping concentration of $7 \times 10^{19} \text{ cm}^{-3}$ at room temperature, i.e., nearly all energy states below the Γ valley in the indirect L valleys are occupied with equilibrium extrinsic electrons. This indirect valley state filling effect makes germanium an effective direct bandgap material since it forces the injected electrons to occupy higher energy states in both the direct Γ valley and the indirect L valleys under carrier injection. Since the radiative recombination rate of the direct transition in Ge is four to five orders of magnitude higher than that of the indirect transitions, the injected electrons in the Γ valley are depleted much faster than those in the L valleys. In order to maintain the quasi-equilibrium of electrons in the conduction band, the electrons in the L valleys populate the Γ valley following intervalley scattering. This process results in further radiative recombination via efficient direct transitions. Therefore, the portion of the injected electrons in the direct Γ valley,

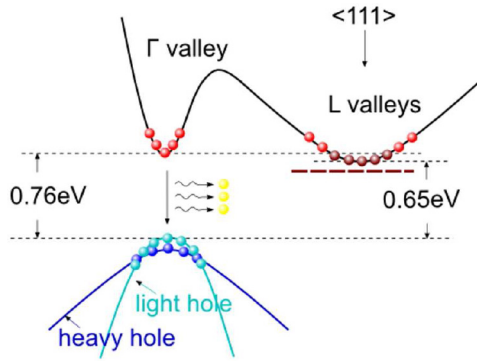


Fig. 3. Band structure and carrier occupation in the conduction and valence bands of germanium with 0.25% tensile strain and $7 \times 10^{19} \text{ cm}^{-3}$ n-type doping concentration under carrier injection. Light red dots and dark red dots represent the injected electrons and the thermally activated extrinsic electrons, respectively. Light blue dots and dark blue dots represent the injected light hole and heavy hole, respectively.

which contributes the direct radiative recombination, is significantly increased.

The band structure and the carrier occupation of germanium with 0.25% tensile strain and $7 \times 10^{19} \text{ cm}^{-3}$ n-type doping concentration under carrier injection are schematically shown in Fig. 3. The occupation of the injection electrons in the direct Γ valley benefits from both the strain-induced bandgap shrinkage and doping-induced indirect L valleys states filling by extrinsic electrons. Most of the injected carriers in the direct Γ valley contribute to the direct-gap light emission due to the fast direct band-to-band transition rate, while the injected carriers in the indirect L valleys recombine nonradiatively. The effect of n-type doping on the enhancement in direct-gap spontaneous emission has been clearly shown in photoluminescence studies [4]–[6].

III. DIRECT-GAP GAIN IN GERMANIUM

While it is easy to understand the positive impact of tensile strain and n-type doping on direct-gap light emission as a result of the increased occupation of injected electrons in the direct Γ valley, the effect of doping on net gain in germanium is not a trivial conclusion because high concentration of extrinsic carriers also introduce optical loss from free carrier absorption. Therefore, the net effect is determined by the competition between the optical gain enhancement from indirect valley states filling and the optical loss from additional free carrier absorption. In our previous modeling work [3], it has been shown that n-type doping is favorable in achieving net gain and laser action. This conclusion can be understood by the following analysis. If intrinsic germanium is used for lasing in order to achieve the necessary population inversion of the direct Γ valley electrons, a very high injection level is required to pump electrons to both the direct Γ valley and the lower energy indirect L valleys. In the mean time, an equal number of holes are also injected into the material. The occurrence of net gain depends whether the optical gain at this certain population inversion level can overcome the optical loss from free carrier absorption contributed by both the injected electrons and holes. However, if n-type doped germanium is used instead, since the energy states (below the

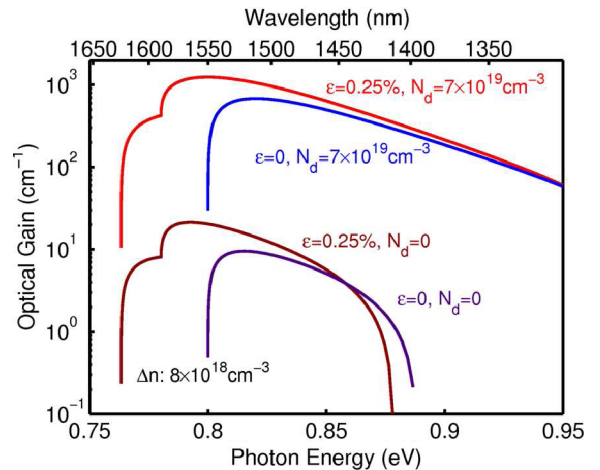


Fig. 4. Comparison of the calculated optical gain spectra of germanium at room temperature near the direct bandgap, using all combinations of tensile strain and n-type doping. The injected excess carrier density (Δn) is $8 \times 10^{18} \text{ cm}^{-3}$.

minimum energy of the direct Γ valley) in the indirect L valleys are already filled by extrinsic electrons, a much lower injected carrier density is needed to achieve the same population inversion level. This advantage leads to much less injected holes, and subsequently, less total free carrier absorption. Furthermore, it has been shown that free hole absorption is about four to six times larger (in the 10^{19} cm^{-3} carrier concentration range) than the free electron absorption near the direct bandgap energy of germanium [21], [22]. Therefore, the free carrier absorption is reduced by more than 80% by using n^+ germanium instead of intrinsic germanium. With a significant reduction in optical loss, net gain is much easier to achieve in doped germanium than in intrinsic germanium, although compared to intrinsic direct bandgap materials like GaAs, a relatively lower net gain is expected because of free carrier absorption from extrinsic electrons.

The effect of tensile strain and n-type doping on the enhancement of optical gain in germanium at room temperature is shown in Fig. 4. The calculation of optical gain is based on the direct band-to-band transition model including optical absorption data measured from our germanium materials. More details on the modeling can be found in our previous work [3]. The shoulders at 0.76 eV for strained germanium represent the optical transition between the separated light-hole band and the direct Γ valley. It can be seen that the optical gain of $7 \times 10^{19} \text{ cm}^{-3}$ doped germanium is over two orders of magnitude larger than that of intrinsic germanium at any photon energy for both the unstrained and strained cases. A moderate tensile strain of 0.25% does not enhance the optical gain by orders of magnitude since the strain level (0.25%) is relatively low compared to the level that leads to direct bandgap germanium (1.8%). Nevertheless, it does increase the optical gain by a factor of 2 and broadens the optical gain spectrum by shifting the optical gain cutoff to lower photon energies (or longer wavelengths), thus resulting in a peak optical gain at about 0.8 eV (1550 nm), which is desirable for many applications. All the optical gain spectra are

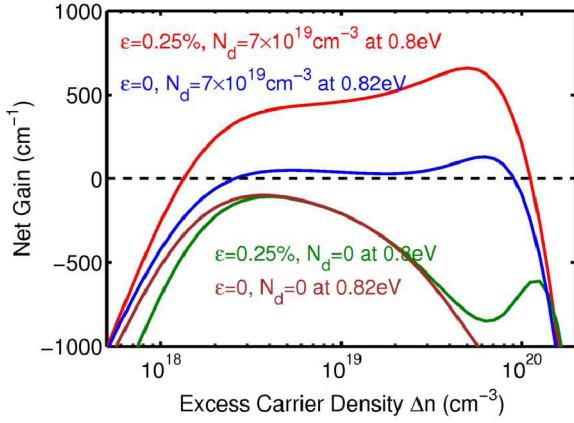


Fig. 5. Comparison of the calculated net gain versus injected excess carrier density Δn in germanium at their peak gain photon energies, using all combinations of tensile strain and n-type doping.

calculated at an $8 \times 10^{18} \text{ cm}^{-3}$ injected carrier density (Δn). At 0.8 eV (1550 nm), tensile-strained n⁺ germanium exhibits a peak optical gain of about 1000 cm^{-1} , which is comparable to direct bandgap material.

As we discussed before, free carrier absorption introduces optical loss that needs to be taken into account to calculate net gain in materials. The calculated net gain, which is the difference between the optical gain and the free carrier absorption, is shown in Fig. 5 for strained and unstrained differently doped germanium. Because the bandgap differs for strained and unstrained germanium in order to compare the optical gain for each case, we choose a photon energy at which the optical gain peaks for a $1 \times 10^{19} \text{ cm}^{-3}$ injected carrier density. It can be clearly seen that the overall effect of n-type doping is beneficial for achieving net gain in germanium. In n-type germanium, net gain can be obtained at injected carrier densities above 10^{18} cm^{-3} even without tensile strain. Net gain from doped germanium is increased from less than 100 cm^{-1} to more than 500 cm^{-1} by introducing 0.25% tensile strain. At very high injected carrier densities above 10^{20} cm^{-3} , net loss occurs because optical gain starts to saturate as a result of complete population inversion and failure to overcome the increasing free carrier absorption. Without n-type doping, the significantly reduced optical gain is not able to overcome the free carrier absorption at any injected excess carrier density, which explains why researchers have never observed net gain from bulk germanium. By using the tensile strain and n-type doping, the onset of net gain has been observed and reported very recently [7].

The calculated net gain spectra of 0.25% tensile-strained, $7 \times 10^{19} \text{ cm}^{-3}$ n-type doped Ge at room temperature for different injected carrier densities are shown in Fig. 6. It can be seen that as high as 400 cm^{-1} net gain can be achieved with a relatively low injected carrier density of $2 \times 10^{18} \text{ cm}^{-3}$, while more than 1000 cm^{-1} net gain is feasible with higher injection levels. The net gain spectrum extends over more than 100 nm for all but the lowest injection level. Increased strain will shift the gain spectrum toward longer wavelengths. The shoulder that was observed for longer wavelengths in Fig. 4 disappears because

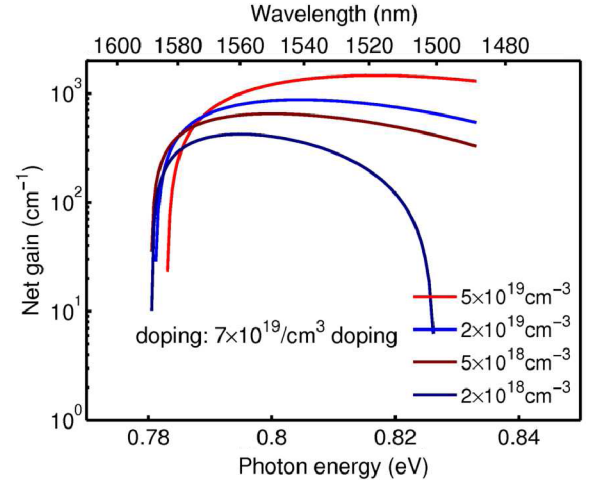


Fig. 6. Room temperature net gain spectrum of 0.25% tensile-strained, $7 \times 10^{19} \text{ cm}^{-3}$ n-type doped Ge at different injected carrier densities.

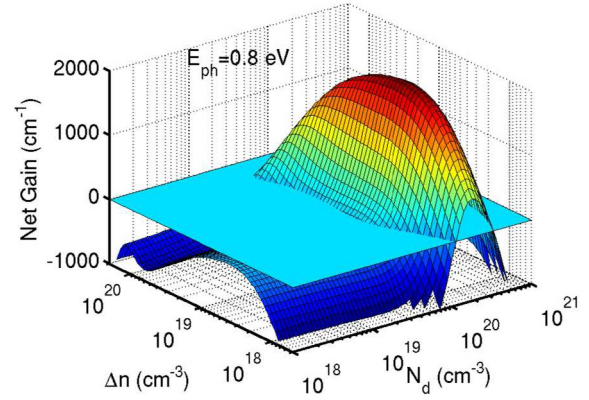


Fig. 7. Dependence of the calculated net gain of 0.25% tensile-strained germanium on the active n-type doping concentration (N_d) as well as the injected excess carrier density (Δn) at 0.8 eV photon energy. The color scheme (from red to blue) represents magnitude of net gain.

the optical gain from the recombination between the light-hole band and the direct Γ valley is not large enough to overcome the free carrier absorption loss. Therefore, net gain can only occur from the energy gap between the heavy-hole band and the direct Γ valley. At this transition, optical gain is higher due to a larger reduced effective mass.

Although n-type doping is essential to achieve net gain in moderately strained germanium, very high doping concentrations introduce too much free carrier absorption and eventually suppresses optical gain. The dependence of net gain from germanium on the n-type doping concentration is calculated at various injected carrier densities, as shown in Fig. 7. It can be seen that a range of n-type doping concentrations and injected carrier densities exists for the occurrence of net gain. Generally, doping concentrations higher than 10^{19} cm^{-3} and excess carrier density higher than 10^{18} cm^{-3} are needed. Compared to the doping concentration we used for the modeling before ($7 \times 10^{19} \text{ cm}^{-3}$), higher active doping concentrations (but below $2 \times 10^{20} \text{ cm}^{-3}$) lead to an even higher peak net gain and lower threshold excess carrier concentration. In reality, the achievable active doping

concentration is limited by the donor solubility, dopant activation, and material processing. The cross section of this 3-D net gain calculation by the zero-net-gain plane gives the threshold boundary surrounding the net gain conditions. This boundary may vary at photon energies other than 0.8 eV, but the general characteristics hold.

Temperature is another factor that affects optical gain and, thus, net gain. The calculated temperature dependence of net gain from 0.25% tensile-strained, $7 \times 10^{19} \text{ cm}^{-3}$ n-type doped germanium is shown in Fig. 7(a). Since the bandgap is also temperature dependent, we calculate the net gain always at photon energies 0.04 eV larger than the direct bandgap at each temperature for fair comparison. The photon energy, chosen at 300 K, is 0.8 eV while the direct bandgap (between the direct Γ valley and the light-hole band) is about 0.76 eV under 0.25% tensile strain. The temperature coefficient data of the direct and the indirect bandgap of germanium used in the calculation can be found in [23].

In Fig. 8(a), net gain is calculated as a function of injected excess carrier density at temperatures between 200 and 400 K. It can be seen that the threshold injected carrier density for net gain is slightly changed with temperature, while the influence of temperature on the net gain above threshold can be divided into two distinct regions. The net gain increases with temperature between threshold and mid- 10^{19} cm^{-3} but it decreases with temperature from mid- 10^{19} cm^{-3} to 10^{20} cm^{-3} . This unusual temperature dependence behavior is a result of the direct-gap optical transition in an indirect bandgap material. Besides the bandgap change with temperature, which we already excluded by using the photon energy $E_{\text{ph}} = E_{\text{g}\Gamma} + 0.04 \text{ eV}$ at each temperature, the influence of temperature on direct-gap optical gain in germanium mainly results from two effects: 1) the proportion of injected excess electrons occupying the direct Γ valley and 2) the proportion of the direct Γ valley electrons contributing to the optical gain at a given photon energy. As we can see in the following discussion, the temperature dependence of these two effects is different. Therefore, the competition between these two effects at different injected carrier densities results in two distinct regions.

The proportion of the injected excess electrons occupying the direct Γ valley changes with temperature because the probability of electrons occupying higher energy states in the direct Γ valley is higher at elevated temperatures, following the quasi-Fermi distribution. Thus, this effect causes the increase in optical gain with temperature and explains the temperature dependence of the net gain at relatively low injected carrier densities. This effect is a unique feature of the direct-gap optical transition in an indirect bandgap material, and it also explains the increase of photoluminescence with temperature shown in [4]–[6].

On the contrary, the second effect, namely the proportion of the direct Γ valley electrons contributing to the optical gain at a given photon energy, increases with the decrease of temperature. This effect is schematically shown in Fig. 8(b), which exhibits the energy distributions of the injected electron and hole densities at high temperature and low temperature. The carrier density distribution is the multiplication of the (quasi) Fermi distribution with the square root density of states at the

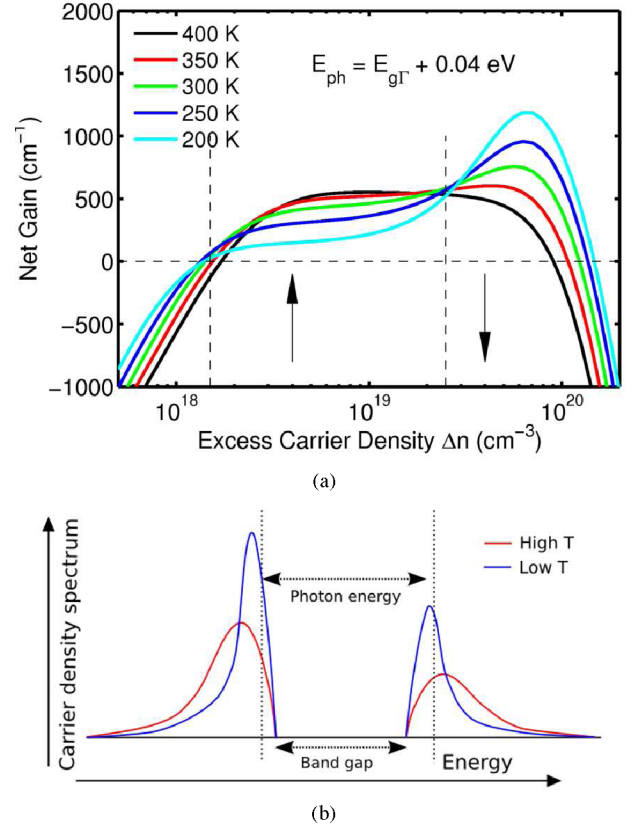


Fig. 8. (a) Calculated net gain of tensile-strained n⁺ Ge versus the injected excess carrier density (Δn) at different temperatures. The temperature dependence of the bandgap is excluded by choosing photon energy of 0.04 eV above the direct bandgap at each temperature for fair comparison. (b) Schematic of energy distribution the direct-gap excess carrier density at high temperature and low temperature.

band edge. The peak width of the carrier density distribution is proportional to the thermal energy (1.5–2 kT). Therefore, the energy distribution of electrons is narrower at the lower temperature. The area of the carrier distribution curve represents the total excess carrier density that is the same for both temperatures at a given injected carrier density. It means that the peak of the distribution at the lower temperature is higher than that at the higher temperature. The stimulated emission rate at a given photon energy is determined by the available electrons and holes at two energy levels, which are shown by the vertical dotted lines, corresponding to the photon energy. We can see that the carrier densities at these two energy levels are higher at the lower temperature; therefore, the optical gain tends to be higher if the total number of injected electrons in the Γ valley is the same. This effect explains the temperature dependence of the net gain at relatively high injected carrier densities.

IV. SILICON GERMANIUM HETEROJUNCTION LIGHT EMITTERS

A critical advantage of the direct-gap light emission in germanium over many Si-based light-emitting materials, such as Er-doped dielectrics, is the ability of electrical injection of excess carriers. We have recently demonstrated the first Ge/Si heterojunction direct-gap LED [8]. In this section, a more

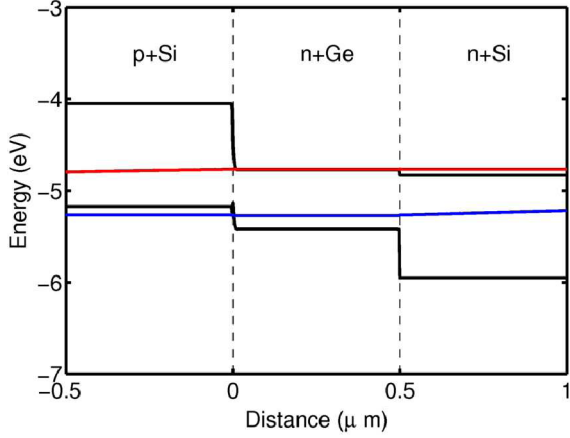


Fig. 9. Band diagram of a $p^+ \text{Si}/n^+ \text{Ge}/n^+ \text{Si}$ diode at 0.5 V forward bias. The doping concentrations in $p^+ \text{Si}/n^+ \text{Ge}/n^+ \text{Si}$ are $1 \times 10^{20} \text{ cm}^{-3}$, $1 \times 10^{19} \text{ cm}^{-3}$, and $1 \times 10^{20} \text{ cm}^{-3}$, respectively. The red line and blue line are the electron and the hole quasi-Fermi levels, respectively.

detailed analysis is presented to address some design principles and a comparison with experimental results.

In the Ge LED, as discussed in [8], the active medium is intrinsic germanium. From the analysis before, we know that germanium has to be doped with n-type impurities in order to enhance the direct-gap light emission efficiency. By replacing the intrinsic Ge with $n^+ \text{Ge}$, the Si/Ge/Si p-i-n diode becomes p-n-n diode. It should be noted that the junction and the active region do not merely occur near the $n^+ \text{Ge}/p^+ \text{Si}$ interface. The whole Ge region is injected with both excess electrons and holes because of the two adjacent heavily doped $p^+ \text{Si}$ and $n^+ \text{Si}$ regions. The band diagram of a 1-D $p^+ \text{Si}/n^+ \text{Ge}/n^+ \text{Si}$ heterojunction at 0.5 V forward bias is simulated using a finite-element method (FEM), and the result is shown in Fig. 9. The simulation combines results from semiconductor device simulator SimWindows with our own carrier distribution calculation considering multiple conduction band valleys. The heterojunction used in the simulation is composed of two $1\text{-}\mu\text{m}$ Si layers (only $0.5 \mu\text{m}$ is drawn) doped p-type and n-type at $1 \times 10^{20} \text{ cm}^{-3}$ each, sandwiching a $0.5\text{-}\mu\text{m}$ Ge-layer-doped n-type at $1 \times 10^{19} \text{ cm}^{-3}$. It can be seen that both electron and hole injection exist in the whole Ge region indicated by the wide separation of the electron and hole quasi-Fermi levels.

The internal quantum efficiency of this heterojunction can be calculated from the ratio of the direct band-to-band radiative recombination rate in the whole active region to the injected carrier rate. The former rate is calculated by substituting the excess carrier density obtained from the simulated quasi-Fermi level into the steady-state rate equation, while the latter rate is calculated from the injection current density. The calculated internal quantum efficiency versus forward bias for both a $p^+ \text{Si}/i\text{-Ge}/n^+ \text{Si}$ heterojunction and a $p^+ \text{Si}/n^+ \text{Ge}/n^+ \text{Si}$ heterojunction is shown in Fig. 10. It can be seen that the EL internal quantum efficiency is improved by over an order of magnitude by substituting intrinsic Ge with $n^+ \text{Ge}$ in the Si/Ge/Si heterojunction. In the $p^+ \text{Si}/n^+ \text{Ge}/n^+ \text{Si}$ heterojunction, internal quantum efficiencies as high as 10% can be achieved, which

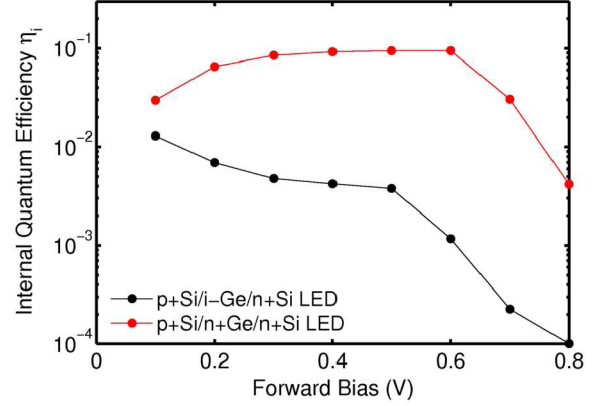


Fig. 10. Calculated direct-gap EL internal quantum efficiency versus forward bias for both a Si/Ge/Si p-i-n heterojunction and a p-n-n heterojunction.

is very promising for an indirect bandgap material. In the calculations before, we have used a conservative direct band-to-band radiative recombination lifetime of 10 ns derived from the measured direct radiative recombination constant in [10]. The Auger coefficient used in this calculation is $10^{-30} \text{ cm}^{-6}/\text{s}$, one order of magnitude higher than reported values for both p-n-n and n-n-p processes [24], [25]. Therefore, the 10% efficiency shown here is the lower limit of Ge direct-gap light emission, and it is promising for the EL efficiency of tensile-strained $n^+ \text{Ge}$ to reach similar efficiencies as direct-gap III-V materials on Si.

The internal quantum efficiencies of both types of diodes decrease above an effective forward bias of 0.6 V because nonradiative recombination processes, mainly Auger recombination, become significant at high injected carrier densities and start to dominate carrier recombination. This process is also represented by the saturation of the EL intensity. Since the injection current keeps increasing rapidly, the internal quantum efficiency decreases.

To compare with experiments, we also derived the internal quantum efficiency from the experimental results of our Ge/Si heterojunction p-i-n diode reported in [8]. The EL collection efficiency, and thus the internal quantum efficiency, can be calculated by carefully considering the geometry of the measurement setup. A multimode fiber (core diameter of $50 \mu\text{m}$) was placed perpendicularly above the LED device ($20 \mu\text{m} \times 100 \mu\text{m}$) top surface to collect the light emission. The air gap between the fiber end and the device surface has to be known to calculate the collection efficiency of the fiber. In the measured EL spectrum in [8], multiple strictly periodic sharp peaks, resulting from the Fabry-Perot resonance corresponding to the air gap, superimposed the direct-gap emission spectrum. Using the periodicity of these peaks, we precisely determined the distance of the air gap, which is equal to $120 \mu\text{m}$. Since the spontaneous light emission escaping from the device surface is completely random and thus angularly uniform, we can obtain the percentage of the light collected by the fiber core area by calculating the solid angle of the core area subtending every point on the device surface. A conservative estimation is to use the same solid angle, which subtends the point right under the center of the fiber core since this solid angle is the largest. With additional

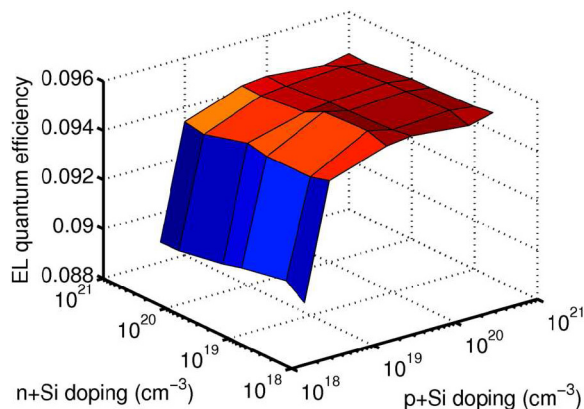


Fig. 11. Calculated EL internal quantum efficiency for a $p^+ \text{Si}/n^+ \text{Ge}/n^+ \text{Si}$ heterojunction versus doping concentrations in the p-type and n-type Si regions at 0.5 V forward bias. The color scheme (from red to blue) represents magnitude of quantum efficiency.

consideration of the transmissivity of the Ge/Si interface, the Si/air interface, the air/silica interface, the total internal reflection effect, and the fiber coupling loss, we calculate that the overall light collection efficiency of the measurement setup is 3.0×10^{-5} . The optical power detected from the collection fiber is ~ 1 nW with an injection current of 50 mA. Using these numbers, the internal quantum efficiency is calculated to be 1×10^{-3} . The simulated result in Fig. 10 suggests an internal quantum efficiency of 4×10^{-3} for the intrinsic Ge heterojunction, which is comparable to the measured result. The remaining difference between these two results is contributed by the modal mismatch between free-space emission light and fiber-guided light, and by possible reduced current injection efficiency from parallel conduction path in real diodes.

As can be seen from the aforementioned analysis, a $p^+ \text{Si}/n^+ \text{Ge}/n^+ \text{Si}$ heterojunction is a good choice for carrier injection in doped germanium gain media. High doping concentrations are used in both silicon regions for building larger quasi-Fermi level separation in the junction. For designing a laser device using this type of junction, these doping concentrations are preferred to be lower because the free-carrier-induced optical absorption in heavily doped materials harms the modal gain in the resonator. Fig. 11 shows the effect of doping concentrations in p-type and n-type Si regions on the EL internal quantum efficiency for the $p^+ \text{Si}/n^+ \text{Ge}/n^+ \text{Si}$ heterojunction. It can be seen that the internal quantum efficiency is more sensitive to the change of the doping concentration in the p-type Si region because the Ge region is n-type; therefore, a heavily doped p-Si region is required for sufficient separation of the quasi-Fermi levels. For a proper heterojunction design, p-Si doped at $5 \times 10^{19} \text{ cm}^{-3}$ and n-Si doped at $1 \times 10^{18} \text{ cm}^{-3}$ can be used.

V. CONCLUSION

In this paper, we follow the work in [3] and discuss in more detail the characteristics of the direct bandgap gain in germanium along with some properties and design guidelines of Ge/Si heterojunction LEDs.

The effects of tensile strain and n-type doping on optical gain and net gain in germanium are calculated. It has been shown that with 0.25% tensile strain, which has already been demonstrated in epitaxial Ge on Si, n-type doping is essential to obtain direct-gap net gain in germanium. Net gain of 500 cm^{-1} can be achieved with an active doping concentration of $7 \times 10^{19} \text{ cm}^{-3}$. Direct-gap spontaneous emission, optical gain, and net gain in Ge increase with doping concentration up to 10^{20} cm^{-3} as a result of the indirect valley states filling effect, which was confirmed by a room-temperature direct-gap photoluminescence study. Direct-gap spontaneous emission, optical gain, and net gain also increase with temperature, except at very high excess carrier densities, due to the thermally activated excess electrons from lower energy states in the indirect L valleys to the direct Γ valley following the quasi-Fermi distribution. This behavior has also been observed in the temperature dependence study of direct-gap photoluminescence in germanium. These doping and temperature dependences are unique optical properties of the direct-gap light emission in an indirect bandgap material. The validation of these properties from these experiments is strong evidence supporting our theory of engineered germanium as a gain medium using its direct bandgap transition.

For electrical carrier injection, we study the properties of a $p^+ \text{Si}/n^+ \text{Ge}/n^+ \text{Si}$ heterojunction diode. Internal quantum efficiencies are calculated for both a doped Ge heterojunction ($p^+ \text{Si}/n^+ \text{Ge}/n^+ \text{Si}$) and an intrinsic Ge heterojunction ($p^+ \text{Si}/i\text{-Ge}/n^+ \text{Si}$). It is shown that the internal quantum efficiency is enhanced by two orders of magnitude by substituting the intrinsic Ge with n-doped Ge. A conservative calculation shows that at least 10% internal quantum efficiency can be achieved from doped Ge heterojunctions. The internal quantum efficiency of the intrinsic Ge heterojunction agrees with the experimentally obtained value from an intrinsic Ge heterojunction LED that we have demonstrated recently. The doping concentrations of both Si regions (n-Si and p-Si) in the Ge/Si heterojunction are also optimized through simulation for low optical loss in silicon without harming the light emission properties.

ACKNOWLEDGMENT

This research was supervised by Dr. G. Pomrenke.

REFERENCES

- [1] M. E. Groenert, C. W. Leitz, A. J. Pitera, V. Yang, H. Lee, R. J. Ram, and E. A. Fitzgerald, "Monolithic integration of room-temperature GaAs/AlGaAs lasers on Si substrates via relaxed graded GeSi buffer layers," *J. Appl. Phys.*, vol. 93, pp. 362–367, 2003.
- [2] A. W. Fang, H. Park, O. Cohen, R. Jones, M. J. Paniccia, and J. E. Bowers, "Electrically pumped hybrid AlGaInAs-silicon evanescent laser," *Opt. Exp.*, vol. 14, pp. 9203–9210, 2006.
- [3] J. Liu, X. Sun, D. Pan, X. Wang, L. C. Kimerling, T. L. Koch, and J. Michel, "Tensile-strained, n-type Ge as a gain medium for monolithic laser integration on Si," *Opt. Exp.*, vol. 15, pp. 11272–11277, 2007.
- [4] X. Sun, J. Liu, L. C. Kimerling, and J. Michel, "Direct gap photoluminescence of n-type tensile-strained Ge-on-Si," *Appl. Phys. Lett.*, vol. 95, 011911, 2009.
- [5] X. Sun, J. Liu, L. C. Kimerling, J. Michel, and T. L. Koch, "Band-engineered Ge as gain medium for Si-based lasers," presented at the Integr. Photon. Nanophoton. Res. Appl., Boston, MA, 2008, Paper IMC5.
- [6] J. Liu, X. Sun, L. C. Kimerling, and J. Michel, "Towards a Ge-based laser for CMOS applications," in *Proc. 5th IEEE Int. Conf. Group IV Photon.*,

- Sorrento, Italy, Sep. 2008, pp. 16–18, (IEEE Catalog No. CFP08GFP-CDR).
- [7] J. Liu, X. Sun, L. C. Kimerling, and J. Michel, “Direct gap optical gain of Ge-on-Si at room temperature,” *Opt. Lett.*, vol. 34, pp. 1738–1740, 2009.
 - [8] X. Sun, J. Liu, L. C. Kimerling, and J. Michel, “Room temperature direct band gap electroluminescence from Ge-on-Si light emitting diodes,” *Opt. Lett.*, vol. 34, pp. 1198–1200, 2009.
 - [9] P. H. Lim, Y. Kobayashi, S. Takita, Y. Ishikawa, and K. Wada, “Enhanced photoluminescence from germanium-based ring resonators,” *Appl. Phys. Lett.*, vol. 93, pp. 041103-1–041103-3, 2008.
 - [10] J. R. Haynes and N. G. Nilsson, “The direct radiative transitions in germanium and their use in the analysis of lifetime,” in *Proc. VIIIth Int. Conf. Phys. Semicond.*, Paris, France, 1964, p. 21.
 - [11] C. G. V. de Walle, “Band lineups and deformation potentials in the model-solid theory,” *Phys. Rev. B*, vol. 39, pp. 1871–1883, 1989.
 - [12] J. Liu, D. D. Cannon, Y. Ishikawa, K. Wada, D. T. Danielson, S. Jongthammanurak, J. Michel, and L. C. Kimerling, “Deformation potential constants of biaxially tensile stressed Ge epitaxial films on Si(100),” *Phys. Rev. B*, vol. 70, pp. 155309-1–155309-5, 2004.
 - [13] Y. Bai, K. E. Lee, C. Cheng, M. L. Lee, and E. A. Fitzgerald, “Growth of highly tensile-strained Ge on relaxed InGaAs by metal-organic chemical vapor deposition,” *J. Appl. Phys.*, vol. 104, pp. 084518-1–084518-9, 2008.
 - [14] Y. Ishikawa, K. Wada, D. D. Cannon, J. Liu, H. Luan, and L. C. Kimerling, “Strain-induced band gap shrinkage in Ge growth on Si substrate,” *Appl. Phys. Lett.*, vol. 82, pp. 2044–2046, 2003.
 - [15] H.-C. Luan, D. R. Lim, K. K. Lee, K. M. Chen, J. G. Sandland, K. Wada, and L. C. Kimerling, “High-quality Ge epilayers on Si with low threading-dislocation densities,” *Appl. Phys. Lett.*, vol. 75, pp. 2909–2911, 1999.
 - [16] D. D. Cannon, J. Liu, Y. Ishikawa, K. Wada, D. T. Danielson, S. Jongthammanurak, J. Michel, and L. C. Kimerling, “Tensile strained epitaxial Ge films on Si(100) substrates with potential application in L-band telecommunications,” *Appl. Phys. Lett.*, vol. 84, pp. 906–908, 2004.
 - [17] Y. Ishikawa, K. Wada, J. F. Liu, D. D. Cannon, H. C. Luan, J. Michel, and L. C. Kimerling, “Strain-induced enhancement of near-infrared absorption in Ge epitaxial layers grown on Si substrate,” *J. Appl. Phys.*, vol. 98, pp. 013501-1–013501-9, 2005.
 - [18] J. Liu, D. D. Cannon, K. Wada, Y. Ishikawa, S. Jongthammanurak, D. T. Danielson, J. Michel, and L. C. Kimerling, “Tensile strained Ge p-i-n photodetectors on Si platform for C and L band telecommunications,” *Appl. Phys. Lett.*, vol. 87, pp. 011110-1–011110-3, 2005.
 - [19] J. Liu, J. Michel, W. Giziewicz, D. Pan, K. Wada, D. D. Cannon, S. Jongthammanurak, D. T. Danielson, L. C. Kimerling, J. Chen, F. O. Ilday, F. X. Kartner, and J. Yasaitis, “High-performance, tensile-strained Ge p-i-n photodetectors on a Si platform,” *Appl. Phys. Lett.*, vol. 87, pp. 103501-1–103501-3, 2005.
 - [20] J. Liu, D. D. Cannon, K. Wada, Y. Ishikawa, S. Jongthammanurak, D. T. Danielson, J. Michel, and L. C. Kimerling, “Silicidation-induced band gap shrinkage in Ge epitaxial films on Si,” *Appl. Phys. Lett.*, vol. 84, pp. 660–662, 2004.
 - [21] W. G. Spitzer, F. A. Trumbore, and R. A. Logan, “Properties of heavily doped n-type germanium,” *J. Appl. Phys.*, vol. 32, pp. 1822–1830, 1961.
 - [22] R. Newman and W. W. Tyler, “Effect of impurities on free-hole infrared absorption in p-type germanium,” *Phys. Rev.*, vol. 105, pp. 885–886, 1957.
 - [23] M. Levinstein, S. Rumyantsev, and M. Shur, Eds., *Handbook Series on Semiconductor Parameters*. Singapore: World Scientific, 1996.
 - [24] R. Conradt and J. Aengenheister, “Minority carrier lifetime in highly doped Ge,” *Solid State Commun.*, vol. 10, pp. 321–323, 1972.
 - [25] S. Marchetti, M. Martinelli, R. Simili, M. Giorgi, and M. Fantoni, “Measurement of Ge electrical parameters by analyzing its optical dynamics,” *Phys. Scr.*, vol. 64, pp. 509–511, 2001.

Xiao Chen Sun (M’09) received the B.S. degree in physics from Peking University, Beijing, China, in 2004, and the Ph.D. degree in materials science and engineering from Massachusetts Institute of Technology, Cambridge, in 2009.

He is currently with Massachusetts Institute of Technology. His current research interests include the areas of silicon photonics, integrated optoelectronics, optical communication and interconnects, and photovoltaics.

Jifeng Liu (M’07) received the B.S. and M. S. degree in materials science and engineering from Tsinghua University, Beijing, China, and the Ph.D. degree in materials science and engineering from Massachusetts Institute of Technology (MIT), Cambridge, in 2006.

He is currently a Postdoctoral Associate at the Microphotonics Center, MIT. His current research interests include GeSi-based active optoelectronic devices for electronic and photonic integration on silicon, including GeSi photonic modulators, light emitters, and photodetectors integrated with high-index-contrast waveguides, and also photovoltaic and thermophotovoltaic (TPV) devices for clean energy applications, including Ge/Si TPV cells and photonic structures for light trapping and efficiency enhancement in thin-film solar cells.

Lionel C. Kimerling (M’89) received the B.S. degree in metallurgical engineering and the Ph.D. degree in materials science from Massachusetts Institute of Technology (MIT), Cambridge, in 1965 and 1969, respectively.

He was formerly the Head of the Materials Physics Research Department, AT&T Bell Laboratories, Holmdel, NJ. He is currently the Thomas Lord Professor of Materials Science and Engineering at MIT, where he is also the Director of the Materials Processing Center. He is involved in the field of electronic, optical, and optoelectronic materials. His current research interests include silicon processing, photovoltaic cells, environmentally benign integrated circuit manufacturing, and monolithic microphotonic devices and circuits.

Jurgen Michel received the Diploma in physics from the University of Cologne, Cologne, Germany, and the Doctorate degree in applied physics from the University of Paderborn, Paderborn, Germany.

In 1990, he joined Massachusetts Institute of Technology, Cambridge, where he is currently a Principal Research Scientist at the Microphotonics Center. He was a Postdoctoral Member of the Technical Staff at AT&T Bell Laboratories. His current research interests include silicon-based photonic materials and devices and silicon-based photovoltaics. He has authored or coauthored more than 180 scientific papers.